Category Decomposition-based Within Pixel Information Retrieval Method and its Application to Partial Cloud Extraction from Satellite Imagery Pixels

Kohei Arai[1], Yasunori Terayama[2], Masao Moriyama[3]
Faculty of Science and Engineering, Saga University, Saga City, Japan[1, 2]
Faculty of Engineering, Nagasaki University, Nagasaki City, Japan[3]

***Abstract*—Category decomposition-based within pixel information retrieval method is proposed together with its application to partial cloud extraction from satellite imagery pixels. A comparative study was conducted for estimation of the sea surface temperature of the pixel suffered from partial cloud cover within a pixel. Three methods for estimation of partial cloud cover within a pixel, based on the proposed category decomposition-based method with Generalized Inverse Matrix Method: GIMM and well-known Least Square Method: LSM and Maximum Likelihood Method: MLH, were compared. It was found that around 9% of RMS (Root Mean Square) error can be achieved. Also, it was found that estimation accuracy highly depends on variance of representative vectors for cloud and the ocean or observed noise. The experimental results with simulated data show RMS error of GIMM are highly dependent to the noise followed by MLH and LSM. The results also show the best estimation accuracy can be achieved for MLH followed by LSM and GIMM.**

***Keywords*—Category decomposition; information retrieval; cloud cover estimation; Generalized Inverse Matrix Method: GIMM and well-known Least Square Method: LSM and Maximum Likelihood Method: MLH**

I. Introduction

When estimating the sea surface temperature using visible thermal infrared radiometer data such as NOAA (National Oceanic and Atmospheric Administration) / AVHRR (Advance Very High-Resolution Radiometer), MOS-1 (Marine Observation Satellie-1) / VTIR (Visible and Thermal Infrared Radiometer), for example, as is clear from the MCSST (Multi-Channel Sea Surface Temperature) [1] algorithm, there is only a small amount in the pixel. However, the pixels that are likely to have clouds are detected and excluded from the target of sea surface temperature estimation. Especially in the case of MCSST, the acquisition rate of data not covered by clouds is low because the policy of punishing suspicions is strictly checked for this possibility. As a result, many observation day data are required to obtain a good scene in which all pixels are not covered with clouds, which often hinders the estimation of the 10-day average sea surface temperature.

Even if a small cloud exists in the pixel, if the brightness temperature of the cloud can be known and the area occupancy can be estimated, it can be corrected to some extent and used. Assuming that the brightness temperature of this cloud is equal to that of the pixel covered with 100% cloud in the vicinity of the core pixel, the method of estimating the cloud coverage rate will be examined here. That is, with the aim of creating products of average sea surface temperature in a short period of time, we propose a method for estimating the cloud coverage rate in pixels and examine its effect.

In this paper, we take up the method of estimating the class occupancy in pixels proposed so far as a method of estimating the cloud coverage [2]-[8] and show the result of mutual comparison of estimation accuracy. These estimation methods have been proposed to estimate the class mixing ratio of mixed pixels (Mixel) consisting of multiple classes. When applying these to cloud coverage estimation, it becomes a problem to estimate the mixing ratio for the two classes of cloud and sea, and in general, the number of channels of visible thermal infrared radiometer data exceeds this, so the minimum square method is effective. It is considered to work. Therefore, we took up the least squares method that minimizes the square of the estimation error of the observation vector and the square of the estimation error of the mixing ratio. In addition, we conducted a theoretical study of the estimation error of these least square methods, and the estimation error is small.

It is shown that it is possible to use both adaptively so as to become. We propose an "adaptive least squares method" based on that principle and apply the effect to actual data to confirm it. Furthermore, since it is expected that the spectral reflection and radiation characteristics of cloud pixels will vary widely, the maximum likelihood method that takes the variance into consideration was taken up as a comparison target and compared.

In the next section, related research works are described in Section II followed by theoretical background and proposed method in Section III. Experiments and experiments results are mentioned in Section IV and Section V respectively and finally conclusion and work for future is explained in Section VI and Section VII respectively.

II. Related Research Works

As for the related research works to category decomposition, there are the followings,

Maximum likelihood estimation of category proportion among Mixels is conducted [9]. Meanwhile, image classification from category proportions among Mixels is proposed [10]. On the other hand, decomposition of category

mixture in a pixel and its application for supervised image classification is proposed [11].

Category decomposition based on subspace method with learning process is proposed [12] together with category decomposition method for un-mixing of Mixels acquired with spaceborne based visible and near infrared radiometers by means of Maximum Entropy Method: MEM with parameter estimation based on Simulated Annealing: SA [13]. On the other hand, focusing on Mixels located at the boundary between two types of classes, an image decomposition algorithm that uses the class mixture ratio of Mixels and the spatial information of surrounding pixels of Mixels are investigated [14]. Research has also been conducted that adds, but it has not been applied to two or more types of class boundaries. Meanwhile, category decomposition requires an endmember extraction in the spectral space of distributions. When observation data, end member spectra, and content rates are each expressed as a matrix, Mixel decomposition can be regarded as a matrix decomposition problem. Due to physical conditions, all components of the matrix are non-negative values, so by applying non-negative matrix factorization (NMF), the end member spectrum and content can be estimated simultaneously [15]. In the data-driven approach, the material with the estimated endmember spectrum is finally identified by referring to the spectral library and searching for the closest spectrum.

Sea ice concentration estimation method with satellite based visible to near infrared radiometer data based on category decomposition is proposed [16]. Also, category decomposition method based on matched filter for un-mixing of mixed pixels acquired with space borne based hyper-spectral radiometers is proposed [17].

Bi-directional Reflectance Distribution Function: BRDF effect on un-mixing, category decomposition of the Mixel of remote sensing satellite imagery data is estimated [18].

On the other hand, there are the following research works related to cloud overage estimation,

A merged dataset for obtaining cloud free Infrared: IR data and a cloud cover estimation within a pixel for SST retrieval is proposed [19]. Meanwhile, estimation of partial cloud coverage within a pixel is conducted [20].

Comparative study on estimation of partial cloud coverage within a pixel is conducted [21]. On the other hand, adjacency effect of layered clouds estimated with Monte-Carlo simulation is estimated [22].

Evaluation of cirrus cloud detection accuracy of GOSAT/CAI (Green House Gasses Observation Satellite / Cloud and Aerosol Imager) and Landsat-8 with laser radar: lidar and confirmation with CALIPSO (Cloud-Aerosol Lidar and Infrared Pathfinder Satellite Observations) data is conducted [23]. Meanwhile, comparative study on cloud parameter estimation among GOSAT/CAI, MODIS (Moderate Resolution Imaging SpectroRadiometer), CALIPSO/CALIOP (Cloud-Aerosol LIdar with Orthogonal Polarization) and Landsat-8/OLI (Operational Land Imager - Landsat Science) with laser radar as truth data is conducted [24].

Thresholding-based method for rain, cloud detection with NOAA/AVHRR data by means of Jacobi iteration method is proposed [25]. Also, adjacency effects of layered clouds by means of Monte Carlo Ray Tracing: MCRT is investigated [26].

III. Theoretical Background and Proposed Method

A. Category Decomposition and Classification Norms

In order to estimate the maximum occupancy category in Mixel, category decomposition [1] is required to estimate the occupancy rate of each category. Several categorical decomposition methods have been devised [1-6], but in this study, the categorical decomposition is formulated using the maximum likelihood estimation method that takes observation errors into consideration. Using this theory has the advantage that unclassified pixels can be determined to be statistically meaningful.

Mixel's spectroscopic vector: *I*, which is a mixture of information from N categories, is considered to be the linear combination of Pure pixel value: *A* and category occupancy: *B* shown in Eq. (1) plus the observation error vector: ε.

$$I = (I_1, I_2, \dots, I_M)^t = AB + \varepsilon \tag{1}$$

where *Ii*: Observation pixel value of the i-th band, *M*: Number of bands. "t" represents transpose. Furthermore, *A* is expressed as follows:

$$A = \begin{bmatrix} A_{11} & \cdots & A_{1N} \\ \vdots & \ddots & \vdots \\ A_{M1} & \cdots & A_{MN} \end{bmatrix}$$

where *Aij*: i-band of pure pixel value of j-category, $B = (B_1, B_2, \cdots, B_N)^t$, *Bj*: Occupancy of category j. And, $\varepsilon = (\varepsilon_1, \varepsilon_2, \dots, \varepsilon_M)^t$, ε_i: observation error of the i-th band. Here, it is assumed that Aij follows the normal distribution of mean A^*_{ij} and variance σij^2: N (A^*_{ij}, σ_{ij}^2), and ε_i follows N (0, σ_{ei}^2), and the spectroscopic vector 1 is a random variable [4]. Here, if the pixel values of Pure pixels in each category are independent, the observed pixel values of the i-band: *I*, are the average A^*_i represented by Eq. (2) and Eq. (3), and the normal distribution of the variance σ_i^2: N (A^*_i , σ_i^2) is obeyed [7].

$$I_i = A_i^* B \tag{2}$$

$$A_i^* = (A_{i1}^*, \dots, A_{iN}^*)$$

$$\sigma_i^2 = B^t S_i B + \sigma_{ei}^2 \tag{3}$$

$$S_i = diag(\sigma_{i1}^2, \dots, \sigma_{iN}^2)$$

where A^*_{ij}: The average of the pure pixel values of the i-band j category, and σ_{ij}^2: the variance of the pure pixel values of the i band, j-category. It is also the variance of the observation error of the σ_{ei}^2: i band.

Observed pixel value of the i-th band: Probability (likelihood) that *Ii* is observed: *P* (*Ii*) is expressed by Eq. (4).

$$P(I_i) = \frac{1}{\sqrt{2\pi\sigma_i}} e^{-\frac{(I_i - A_i^*)^2}{2\sigma_i^2}} \tag{4}$$

Probability (likelihood) that the spectroscopic vector I is observed (likelihood): $P(I)$ is expressed by Eq. (5), assuming that it is independent between each band.

$$P(I) = \prod_{i=1}^{M} P(I_i) \quad (5)$$

In general, each band of remote sensing data is not independent of each other, so it is necessary to make each band independent by orthogonalization transformation such as principal component analysis as preprocessing. Here, based on the concept of the maximum likelihood estimation method, the solution is to find the probability that the spectral vector is observed: $P(I)$ and the occupancy rate: B I. Here, the occupancy rate: B has the following constraints if the type of category included in Mixel is known.

$$\sum_{j=1}^{N} B_j = 1, B_j \geq 0, (j = 1, \dots, N) \quad (6)$$

The category occupancy (maximum likelihood estimation value) estimated based on this method is expressed as B^*, and the pixels are classified into category K of the maximum element B^*_k in B^*. This method is called the Maximum Proportion Classifier (MPC).

B. Determination of Unclassified Pixels

In image classification methods such as the maximum likelihood method and the shortest distance method, restrictions are set according to those classification norms, and those exceeding the restrictions are regarded as unclassified pixels [8], [9]. This section describes how to determine unclassified pixels according to the maximum occupancy classification norm.

Comparing Mixel and Pure Pixel, Pure Pixel expresses its pixel value by the mean and variance of the classified categories, while Mixel's pixel value is the occupancy rate of each category and their mean and variance. This indicates that Mixel has more independent parameters to express the pixel value of Mixel than Pure Pixel, and Mixel is a concept with a high degree of freedom. With these things in mind, this study proposes the following method for determining unclassified pixels.

The fact that a Mixel can be classified into one category (Mixel can be represented by one category) means that the Mixel can be represented by a model with more constraints (fewer independent parameters) (Pure pixel hypothesis). That's what it means. In such a case, the Pure pixel hypothesis is tested using the model goodness-of-fit test [7], [10], and if the Pure pixel hypothesis holds, it can be classified, otherwise it cannot be classified. It is possible to do. Here, we propose two types of goodness-of-fit test methods.

C. Goodness of Fit Determined by χ^2 Distribution [10]

Suppose there are two models π_1 and π_2, and π_1 is π_2, which is a special case (the number of independent parameters is small). The likelihood ratio of the two models: β is defined by Eq. (7), where P (π) is the likelihood of the model π.

$$a = P(\pi^*_1) / P(\pi^*_2) \quad (7)$$

where, the superscript * represents the maximum likelihood estimator of the model π. Since π^*_1 is a special case of π^*_2, P (π^*_1) ≤ P (π^*_2)), and therefore $\beta \leq 1$ holds. Here, χ^2 of Eq. (8) is defined.

$$\chi^2 = -2 \ln \beta \quad (8)$$

χ^2 asymptotically has a chi-square distribution with $n = n_2 - n_1$ degrees of freedom. Here (n_1 and n_2 are the number of independent parameters of the models π_1 and π, respectively), and the percentile value χ^2 (n) of 100 by α% (α: significance level, $0 < \alpha < 1$) of the chi-square distribution with n degrees of freedom, α) and χ^2 can be compared to test whether π, is significantly inferior to π_2 (χ^2 (n, α) $< \chi^2$).

When this goodness-of-fit test is used to determine unclassified pixels according to the maximum occupancy classification standard, only the maximum occupancy category B^*_k of the most likely estimated value B^* of the occupancy obtained by categorization of π_1 Pire pixel ($B^*_K = 1$, occupancy of other elements is 0), $P(\pi_1)$ is obtained from Eq. (4) and Eq. (5), then π_2 is Mixel, and B* is used (4).), (5) to find P (π_2), and Eq. (7) and Eq. (8) to find χ^2. Here, from the constraint condition of Eq. (6), the number of independent parameters of PURE PIXEL is 0, and the number of independent parameters of Mixel is N-1 (N: number of categories), so $n=N$-1. Therefore, the significance level α (right side test) of the test is determined, χ^2 (N-1,α) is calculated, compared with χ^2, and the unclassified pixels are χ^2 (N-1),α) ≤ χ^2: Unclassified χ^2 (N-1,α)> χ^2: Determined to be classified in the maximum occupancy category. Since χ^2 becomes larger as the likelihood ratio β is smaller (the likelihood is smaller when it is a pure pixel), the number of unclassified pixels increases as the significance level is increased (χ^2 (N-1, α) becomes smaller).

D. Goodness of Fit Test by AIC [10],[11]

Similar to the goodness-of-fit test based on the χ^2 distribution, there are two models, π_1 and π, and π_1 is a special case of π_2. If $P(\pi)$ is the likelihood of the model π, then AIC (Akaike's Information Criterion) is defined by Eq. (9).

$$AIC = 2(n - 2)\ln\{P(\pi^*)\} \quad (9)$$

where n is the number of independent parameters of the model, and the superscript * is the maximum likelihood estimator of the model. Here, the model that minimizes the AIC in Eq. (9) is selected. Similar to the goodness-of-fit test based on the χ^2 distribution, π_2 is Mixel (number of independent parameters: N-1), π_1 is Pure pixel (number of independent parameters: 0) containing only the maximum occupancy category, and AIC is Eq. (4), (5), (9), if the AIC obtained from the case of Pure pixel is smaller than the AIC obtained from the case of Mixel, it is judged that it can be classified and classified into the maximum occupancy category. If not, it is regarded as an unclassified pixel.

IV. Experiments

A. Simulation of Pure Pixel Data

The validity of the above theory will be confirmed by the following data and simulation according to the procedure.

Using TM data around Lake Ashino-ko in Japan, which was acquired by LANDSAT 5 on June 6, 1987, residential areas, bare land, grasslands, coniferous forests, and broad-

leaved forests, which are typical categories of this area, were ed as the grand truth area. It is extracted using vegetation maps and aerial photographs [12]. Then, in order to make each band independent, all bands except the thermal band (band 6) were analyzed for principal components, and the first and second principal components were quantized into eight bits and used for categorization. Table I shows the eigenvalues, eigenvectors, and contribution ratio of each principal component. Table II shows the average and variance of the pixel values of each category Pure pixel.

TABLE I. EIGENVALUE, EIGENVECTOR AND CONTRIBUTION OF THE TEST DATA. PC, E-VALUE, E-VEC. AND CONT. MEAN PRINCIPAL COMPONENT, EIGENVALUE, EIGENVECTOR AND CONTRIBUTION, RESPECTIVELY

	PC1	PC2	PC3	PC4	PC5	PC6
E-value	5.47	0.49	0.03	0.01	0.00	0.00
Band 1	0.41	-0.33	0.00	-0.83	0.13	-0.08
Band 2	0.42	-0.26	-0.27	0.32	-0.35	-0.68
Band 3	0.42	-0.29	-0.12	0.19	-0.42	0.72
Band 4	0.36	0.75	-0.53	-0.12	0.07	0.06
Band 5	0.41	0.39	0.79	0.02	-0.23	-0.09
Band 7	0.42	-0.16	0.09	0.39	0.79	0.06
Cont.	0.91	0.08	0.01	0.00	0.00	0.00

TABLE II. AVERAGE AND VARIANCE OF THE PURE PIXEL DATA. AV AND VR MEANS AVERAGE AND VARIANCE, RESPECTIVELY. THE NUMBERS 1 TO 5 SHOW THAT THE CATEGORIES OF RESIDENTIAL AREA, BARE SOIL, GRASS LAND, NEEDLE LEAF TREE AND BROAD LEAF TREE, RESPECTIVELY

		1	2	3	4	5
A	PC1	97.8	162.4	127.3	60.9	107.8
V	PC2	62.2	135.1	162.0	100.9	187.7
V	PC1	160.4	841.1	185.7	94.0	178.2
R	PC2	309.9	681.3	430.4	329.3	586.2

B. Simulation of Mixel Data

Mixel data of 36 types (six types of variances by six types of observation error) were created by the procedure shown below,

1) Category occupancy rate: Using the uniform random numbers of [0,1), 100 points of category occupancy are created based on the constraint condition of Eq. (6).

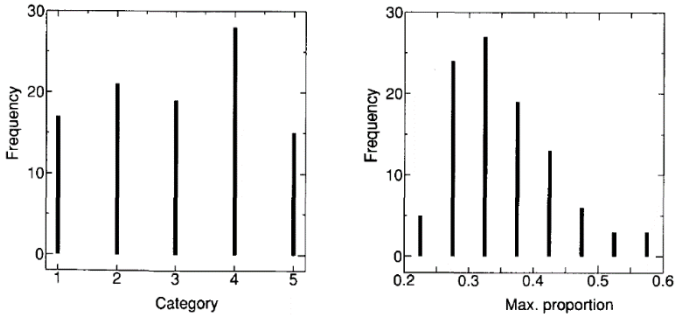

Fig. 1. Characteristics of the truth data. (a) Histogram of the maximum proportion category. The categories number 1 to 5 correspond to the categories of Residential area, Bare soil, Grass land, Needle leaf tree and Broad leaf tree, respectively. (b) Histogram of the maximum proportion.

Fig. 1(a) and Fig. 1(b) show the distribution of the maximum occupancy category and the distribution of the maximum occupancy, respectively.

2) Pure pixel value (training data): Pure pixel values according to the mean and variance of each category are created for each band using normal random numbers. At this time, in order to confirm the influence of the variance of the Pure pixel value, the Pure pixel value is created by multiplying the variance of each category and each band by 2.0, 1.0, 0.8, 0.6, 0, 4, 0.2, respectively.

3) Observation error: The standard deviation σ_{ei} of the observation error in each band is 0,2,4,6,8,10 [Count]. The observation error is created using normal random numbers.

4) Mixel dataset: From the data of (1)-(3), 100 points of Mixel spectroscopic vectors are created under each condition according to Eq. (1).

C. Verification Details

The 30 types of Mixe1 data sets created by the above method were categorized using the grid search method [13] with a side length of 1/64. This solution creates a mesh with a side length of 1/64 in the solution space (N-1 dimensional hyperplane) given by Eq. (6) and uses the training data given at each point of the mesh and the observed spectral vector. The likelihood given by Eq. (5) is calculated, and the point that gives the maximum likelihood is the solution.

As for the solution of the nonlinear optimization problem, all high-speed calculation methods such as Newton's method are methods for finding extreme values, not methods for finding maximum / minimum values. In this study, in order to avoid a decrease in the accuracy of categorization due to algorithm restrictions, categorization was performed by the lattice search method without using high-speed calculation. In actual applications, it is necessary to develop accurate and high-speed algorithms, which will be an issue for the future.

From the estimated value of the category occupancy and the estimated maximum occupancy category obtained here, the following items are verified together with the truth data of the category occupancy in Eq. (1) Category occupancy rate.

D. Comparison of Goodness-of-Fit Test by χ^2 Distribution and Goodness-of-Fit Test by AIC

In order to compare the two unclassified pixel determination methods and confirm the effect of the goodness-of-fit test based on the χ^2 distribution on the classification accuracy of water a, the goodness-of-fit test by AIC and the significance level α were set to 1, 5, 10%. Classification was performed using MPC to which the method for determining unclassified pixels by the goodness-of-fit test was applied. In this case, the same method for determining unclassified pixels is applied to the truth data of the occupancy rate of Eq. (1) Category occupancy rate, and only the classifiable pixels are extracted, and the classifiable pixels obtained here, and their maximum occupancy category are classified and was used as the truth data of the category to be classified.

E. Comparison with Maximum Likelihood Method

The 36 types of Mixel datasets created in steps 3 and 2 were classified by the maximum likelihood classifier (MLC) and compared with the classification results by MPC. In this case, the following two types of unclassified pixel determination methods were used. We used to extract classifiable pixels.

1) Not classified if the log-likelihood is -20 or less.

2) If the Mahalanobis distance to the target category is three times or more the maximum standard deviation of that category, it is unclassified.

Here, as in Eq. (1) Category occupancy rate, the true data of the occupancy rate is classified by MPC using the unclassified pixel determination method by AIC, and the classifiable pixels and their maximum occupancy rate categories are extracted and classified and the truth data of the category to be used.

V. Experimental Results

A. Comparison of Goodness-of-Fit Test by χ^2 Distribution and Goodness-of-Fit Test by AIC

The occupancy rate estimated by categorical decomposition and the likelihood used to determine unclassified pixels are affected by the variance term σ_1 in Eq. (3). Since the variance term is determined by the category occupancy rate, the variance of the Pure pixel value, and the variance of the observation error, the average variance AVG [σ] of Eq. (10) is obtained for each of the 30 types of Mixel data (100 points each) and used. The characteristics of each Mixel dataset are shown.

$$AVG[\sigma] = \frac{1}{100}\sum_{k=1}^{100}\{\frac{1}{M}\sum_{i=1}^{M}(B_k^t S_i B_k + \sigma_{ei}^2)\} \quad (10)$$

First, in order to confirm the accuracy of categorization, the root mean square error RMSE between the occupancy rate B^* and the true value B estimated from each Mixel data set is obtained from Eq. (11), and the mean variance AVG [σ] is used. The relationship is shown in Fig. 2.

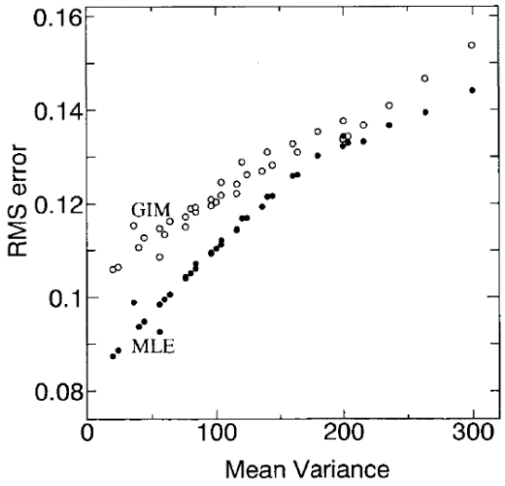

Fig. 2. The relationship between the mean variance and the root mean square error of the estimated category proportions from maximum likelihood estimation (MLE) and generalized inversion matrix (GIM).

Here, the results when the general inverse matrix, which is a typical conventional categorical decomposition method, is used are also shown.

$$RMSE = \frac{1}{100}\sum_{k=1}^{100}\{\frac{1}{N}(B_k^* - B_k)^t(B_k^* - B_k)\} \quad (11)$$

In both methods, it was confirmed that as the mean variance increases (the variance of the Pure pixel value and the observation error variance increase), the RMSE increases and the accuracy of categorization decreases. In addition, the generalized inverse matrix does not take into account the variation in the Pure pixel values of each category [1], indicating that the estimation accuracy is lower than that of the maximum likelihood estimation method.

Next, in order to clarify the relationship between the goodness-of-fit test method for determining unclassified pixels and the degree to which the Mixel data set created by the above method is judged to be classifiable, these unclassified truth data are included in the truth data of the occupancy rate. The relationship between the number of classable pixels obtained by applying the classification pixel determination method and the average variance was obtained. The results are shown in Fig. 3.

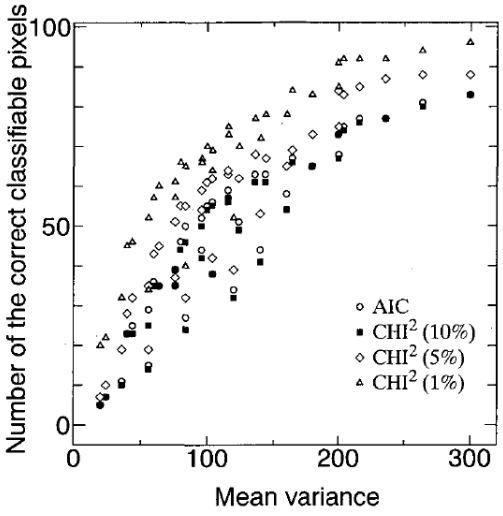

Fig. 3. The relationship between the mean variance and the number of selected classifiable pixel from the truth data of the proportion from Chi square and AIC method.

As the mean variance increases, the likelihood P represented by Eq. (4) and Eq. (5) becomes a gentle function, so the number of pixels judged to be classifiable by all goodness-of-fit test methods increases. In addition, it was confirmed that the number of pixels judged to be classable decreases as the significance level increases in the goodness-of-fit test using the χ^2 distribution, and the goodness-of-fit test using the AIC is a goodness-of-fit test using the χ^2 distribution with the significance level set to 10%.

It was confirmed that almost the same result as the above was obtained. Here, as classification accuracy verification, from the classification result using the estimated value of the category occupancy rate, it was judged that (a) the number of pixels judged to be categorizable and (b) the truth data of the occupancy rate could be classified. The number of pixels

determined to be unclassified by the estimated value (number of error pixels of the first type), (c) Pixels determined to be unclassified by the truth data of the occupancy rate but determined to be classifiable by the estimated value The number (the number of pixels of the type II error) and (d) the classification correctness: (the number of pixels correctly classified) / (the number of pixels judged to be classifiable) were calculated. The results are shown in Fig. 4(a) to Fig. 4(d).

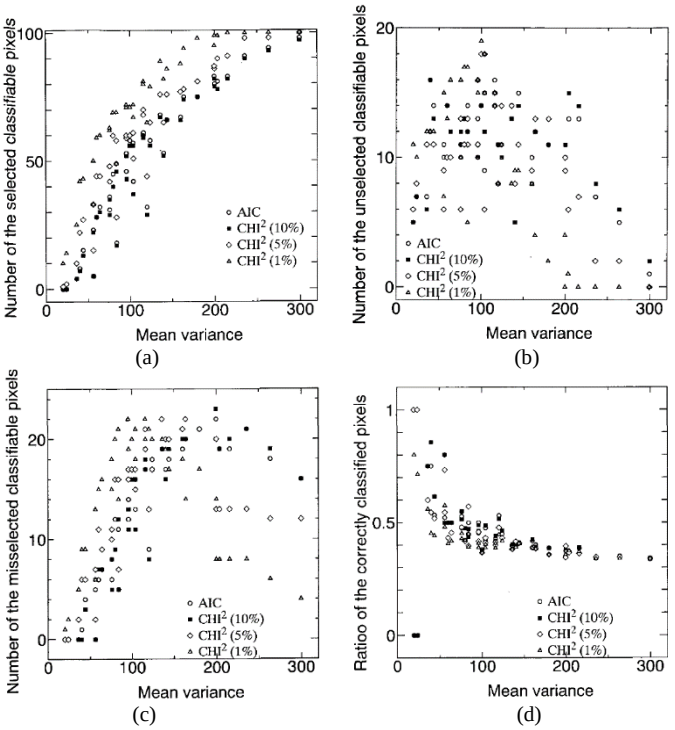

Fig. 4. The classification results from Maximum proportion classifier from various unclassified limits. (a) The number of selected classifiable pixels. (b) The number of unselected classifiable pixels. (c) The number of mis-selected classifiable pixels. (d) The ratio of correctly classified pixels.

It was confirmed that the number of pixels judged to be classable increased as the mean variance increased and decreased as the significance level increased, as in the case obtained from the truth data of the occupancy rate, and the goodness-of-fit test by AIC was significant. It was confirmed that almost the same result as the goodness-of-fit test based on the χ^2 distribution when the level was set to 10% was obtained.

It was confirmed that the number of pixels of the type I error increases with the increase of the average variance up to about 100, and then converges or decreases comparatively gently. In the goodness-of-fit test using the χ^2 distribution, when the significance level was reduced, the number of pixels of type I errors tended to decrease rapidly when the mean variance increased. This can be explained by the fact that the number of pixels judged to be categorizable increases as the significance level increases. In this case as well, the goodness-of-fit test by AIC gave almost the same results as the goodness-of-fit test by χ^2 distribution when the significance level was 10%.

It was confirmed that the number of pixels of the type II error increases as the average variance increases. It was also confirmed that when the significance level was reduced in the goodness-of-fit test using the χ^2 distribution, the number of pixels of the type II error decreased when the mean variance increased. This is because if the significance level is reduced, it is judged that it can be almost classified even when applied to the truth data of the occupancy rate. In this case as well, the goodness-of-fit test by AIC gave almost the same results as the goodness-of-fit test by χ^2 distribution when the significance level was 10%.

The classification correctness tended to decrease as the mean variance increased, and it was confirmed that the difference in the correctness due to the difference in the goodness-of-fit test method also decreased as the mean variance increased. In this case, if the number of pixels determined to be classable is 0, the correctness rate is set to 0.

B. Comparison with Maximum Likelihood Method

The result of classifying the above 30 Mixel datasets by the maximum likelihood method (MLC) with two unclassified limits (log-likelihood and Mahalanobis distance) and the number of unclassified pixels using the AIC goodness-of-fit test. A comparison of the classification results by MPC to which the determination method is applied is shown.

As classification accuracy verification, from the classification result using the estimated value of the category occupancy rate, (a) the number of pixels judged to be categorizable (b) the truth data of the occupancy rate was judged to be categorizable, but the estimated value is not yet.

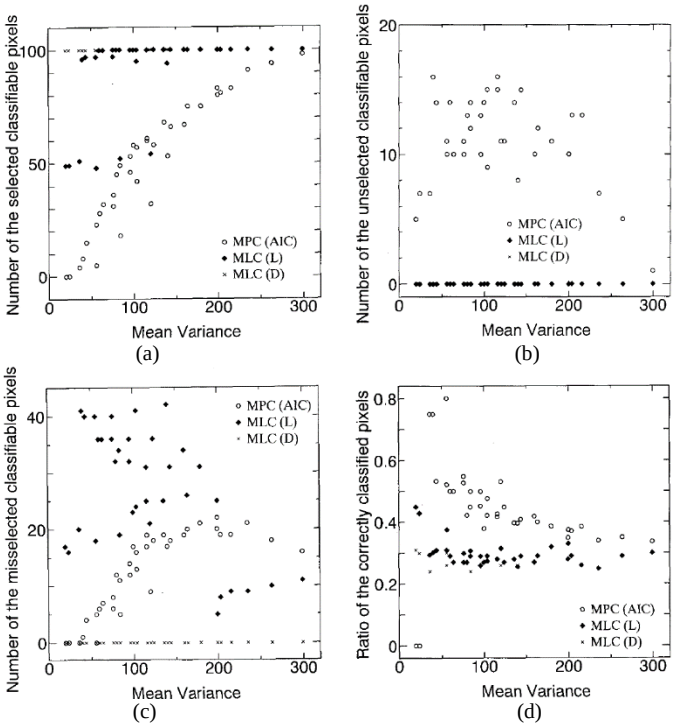

Fig. 5. Comparison of classification result from Maximum proportion classifier with AIC based unclassified limit: MPC(AIC), Maximum likelihood classifier with likelihood based unclassified limit: MLS(L) and with distance based unclassified limit: MLC(D). (a) The number of selected classifiable pixels. (b) The number of unselected classifiable pixels. (c) The number of mis-selected classifiable pixels. (d) The ratio of correctly classified pixels.

The number of pixels determined to be classified (type I error pixels), (c) The number of pixels determined to be unclassified in the truth data of the occupancy rate but determined to be classified by the estimated value (second) (Number of pixels with type error), (d) Classification correctness: (Number of pixels correctly classified) / (Number of pixels judged to be classifiable) were calculated. The results are shown in Fig. 5(a) to Fig. 5(d).

It was confirmed that the number of pixels judged to be classable by the maximum likelihood method applying the unclassified pixel determination method using the likelihood increased with the increase of the average variance, but the average variance was about 150, and all of them. It is judged that it can be classified.

Fig. 5(a) shows that when the maximum likelihood method is applied to Mixel, which targets categories with large variance, it is difficult to set the unclassified limit. The effect of the unclassified limit setting value appears in the error analysis of the above, especially in the number of pixels of the type I and type II errors.

The number of error pixels of the first type (the number of pixels that are determined to be unclassified pixels even though they can be dispersed) is 0 because the number of pixels that are determined to be classifiable in the most probable method is large. The number of error pixels (the number of pixels judged to be classifiable even though they are unclassified pixels) tends to increase when the average variance is small (200 or less) compared to when MPC is used. This indicates that the maximum likelihood method increases misclassification when the mean variance is small (the variance of the Pure pixel value is large, and the variance of the observation error is large) when compared with the result of classification by MPC.

The classification correctness rate when the maximum likelihood method is used is about 30%, which is not so affected by the mean variance. On the other hand, the results by MPC show that the correctness rate decreases as the mean variance increases, but the correctness rate is generally higher than that by the maximum likelihood method. These results represent the limits of the maximum likelihood method, which assumes that the pixel is a pure pixel, and show the usefulness of the proposed method.

In addition, the unclassified limit in the maximum likelihood method does not mean that the likelihood, or the variance and classifiable of a particular category, is fully meaningful, and in addition, the parameters of unclassified pixel determination are for each category. Since it is sensitive to the dispersion of Pure pixel values, it is difficult to determine the optimum parameters.

On the other hand, the method of determining unclassified pixels by the goodness-of-fit test corresponding to MPC proposed in this study is based on the hypothesis test that the Mixel can be regarded as a pure pixel, and in addition, the pure pixel of each category. It is effective and easy to use because it is insensitive to pixel values. Furthermore, since the goodness-of-fit test by AIC is a method that excludes the arbitrariness of the significance level, it has the advantage that unclassified pixels can be uniquely determined.

VI. Conclusion

The following conclusions can be drawn from the above results. Considering that each pixel in remote sensing is a Mixel, we propose a maximum occupancy classification norm that classifies pixels into the maximum occupancy category, and in addition, a method for determining unclassified pixels based on the goodness of fit of the pixel as a pure pixel. It showed that from the simulation of artificially creating Mixel, the result that the proposed method has better classification accuracy than the maximum likelihood method was obtained, and the limit of the maximum likelihood method and the effectiveness of the proposed method were shown.

We also proposed two methods for determining unclassified pixels by the goodness-of-fit test according to the proposed method, one based on the χ^2 distribution and the other based on the AIC, and it was confirmed that there was not much difference between the two. From this, it was concluded that the χ^2 distribution should be used when the number of classified pixels should be adjusted according to the user's situation, and the AIC should be used when the significance level should be excluded.

Since this method takes a long time to calculate at present, it is used as a secondary application such as a remedy for pixels determined to be unclassified in the maximum likelihood classification, or classification of clouds and the sea in the sea area. It can be used as a classification method when the number of categories is small.

VII. Future Research Works

In the future, we plan to develop a high-speed calculation method for maximum likelihood estimation of category occupancy so that it can be used as a general classification method.

Acknowledgment

The author would like to thank Professor Dr. Hiroshi Okumura and Professor Dr. Osamu Fukuda for their valuable discussions.

References

[1] Corniilon, P. et al ,. Sea Surf aco Tcmpcraturo Products for the Oceano graphic Scientific Research Community, Joint Oceanographic Institutions. Inc. p.1-36.1989.

[2] Inamura, 1987. Analysis of remote sensing image data based on category decomposition, Journal of the Institute of Electronics, Information and Communication Engineers, vo1.J70-C, No.2, pp.241-250 1987.

[3] Rikimaru, Uegami, Oshima, 1988. Development of a simple estimation method for intra-pixel spectroscopic information, Journal of the Japanese Society of Photometric Survey, vol.27, No.6, pp.23-34, 1988.

[4] Matsumoto, Fujiku, Tsuchiya, Arai, Category based on maximum likelihood estimation method, decomposition, Journal of Photogrammetry, Japan, Vol.30, No.2, pp.25-34,1991.

[5] Ito, Fujimura, Area Ratio Estimate by Pixel Category Decomposition, Proceedingseedings of the Society of Instrument and Control Engineers, Vol.23, No.8, pp.20-25,1987.

[6] Kohei Arai,and Y. Terayama. 1990. A Method for Proportion Estimate by Means of inversion Problem Solving, Proceedingseedings of the ISPRS Mid-Term Symposium, Commission Vil, WP-1-1, 1990.

[7] Kohei Arai, Terayama, Matsumoto, Fujiku, Tsuchiya, 1991, Context classification with class mixing ratio estimation in adjacent boundary pixels, Journal of the Remote Sensing Society of Japan, Vol.11, No.4, pp.21-28, 1991.

[8] Kohei Arai, Estimation of partial cloud coverage within a pixel, 1991. Proceedingseedings of the Pre-ISY International Symposium pp.97-106, 1991.

[9] M.Matsumoto, Y.Terayama and Kohei Arai, Maximum likelihood estimation of category proportion among mixels, Proceedings.of the ISPRS Committee-III, PS-6-8, 1992.

[10] M.Matsumoto, Y.Terayama and Kohei Arai, Image classification from category proportions among mixels, Proceedings.of the ISPRS Committee-VII, PS-9-15, 1992.

[11] M.Matsumoto, Kohei Arai, T.Ishimatsu, Decomposition of category mixture in a pixel and its application for supervised image classification, Proceedings.of the KACC'92, 514-519, 1992.

[12] Kohei Arai and Chen H., Category decomposition based on subspace method with learning proceedingsess, Abstract, COSPAR A1.1, A-00712, 2006.

[13] Kohei Arai, Category decomposition method for un-mixing of mixels acquired with spaceborne based visible and near infrared radiometers by means of Maximum Entropy Method with parameter estimation based on Simulated Annealing, International Journal of Advanced Research in Artificial Intelligence, 2, 4 64-69, 2013.

[14] Makoto Nishida, Yoichi Kageyama, Takashi Soma, Image Resolution Algorithm for Mixed Pixel of Boundary Area, T. IEE Japan, Vol. 116-C, No. 12, 1418-1419, 1996.

[15] Miao, L. and Qi, H.: Endmember extraction from highly mixed data using minimum volume constrained nonnegative matrix factorization, IEEE Trans. Geosci. Remote Sens., Vol. 45, No. 3, pp. 765-777, 2007.

[16] Kohei Arai, Sea ice concentration estimation method with satellite based visible to near infrared radiometer data based on category decomposition, International Journal of Advanced Research in Artificial Intelligence, 2, 5, 7-13, 2013.

[17] Kohei Arai, Category decomposition method based on matched filter for un-mixing of mixed pixels acquired with space borne based hyper-spectral radiometers, International Journal of Advanced Research in Artificial Intelligence, 2, 6, 20-26, 2013.

[18] Kohei Arai, Bi-directional reflectance distribution function: BRDF effect on un-mixing, category decomposition of the mixed pixel (MIXEL) of remote sensing satellite imagery data, International Journal of Advanced Research in Artificial Intelligence, 2, 9, 19-23, 2013.

[19] Kohei Arai, A Merged Dataset for Obtaining Cloud Free IR Data and a Cloud Cover Estimation within a Pixel for SST Retrieval, Asian-Pacific Remote Sensing Journal, Vol.4, No.2, pp.121-127, Jan.1992.

[20] Kohei Arai, Estimation of partial cloud coverage within a pixel, Proceedings.of the Pre-ISY International Symposium, 99-106, 1991.

[21] Kohei Arai, Y.Ueda and Y.Terayama, Comparative study on estimation of partial cloud coverage within a pixel, Proposed adaptive least square method with constraints- Proceedings.of the European ISY Conference, 305-310, 1992.

[22] Kohei Arai, Adjacency effect of layered clouds estimated with Monte-Carlo simulation, Advances in Space Research, Vol.29, No.19, 1807-1812, 2002.

[23] Kohei Arai, Masanori Sakashita, Evaluation of Cirrus Cloud Detection Accuracy of GOSAT/CAI and Landsat-8 with laser Radar: Lidar and Confirmation with Calipso Data, International Journal of Advanced Research on Artificial Intelligence, 5, 1, 14-21, 2016.

[24] Kohei Arai, Masanori Sakashita, Hiroshi okumura, Shuichi Kawakami, Kei Shiomi, Hirofumi Ohyama, Comparative Study on Cloud Parameter Estimation AmongGOSAT/CAI, MODIS, CALIPSO/CALIOP and Landsat-8/OLI with Laser Radar as Truth Data, International Journal of Advanced Research on Artificial Intelligence, 5, 5, 21-29, 2016.

[25] Kohei Arai, Thresholding Based Method for Rain, Cloud Detection with NOAA/AVHRR Data by Means of Jacobi Iteration Method, International Journal of Advanced Research on Artificial Intelligence, 5, 6, 21-27, 2016.

[26] Kohei Arai, Adjacency effects of layered clouds by means of Monte Carlo Ray Tracing, International Journal of Advanced Computer Science and Applications IJACSA, 11, 1, 95-98, 2020.

AUTHOR'S PROFILE

Kohei Arai, He received BS, MS and PhD degrees in 1972, 1974 and 1982, respectively. He was with The Institute for Industrial Science and Technology of the University of Tokyo from April 1974 to December 1978 also was with National Space Development Agency of Japan from January, 1979 to March, 1990. During from 1985 to 1987, he was with Canada Centre for Remote Sensing as a Post Doctoral Fellow of National Science and Engineering Research Council of Canada. He moved to Saga University as a Professor in Department of Information Science on April 1990. He was a councilor for the Aeronautics and Space related to the Technology Committee of the Ministry of Science and Technology during from 1998 to 2000. He was a councilor of Saga University for 2002 and 2003. He also was an executive councilor for the Remote Sensing Society of Japan for 2003 to 2005. He is a Science Council of Japan Special Member since 2012. He is an Adjunct Professor of University of Arizona, USA since 1998. He also is Vice Chairman of the Science Commission "A" of ICSU/COSPAR during 2008 and 2020 then he is now award committee member of ICSU/COSPAR. He is now Visiting Professor of Nishi-Kyushu University since 2021, and is Visiting Professor of Kurume Institute of Technology (Applied AI Laboratory) since 2021. He wrote 87 books and published 700 journal papers as well as 570 conference papers. He received 66 of awards including ICSU/COSPAR Vikram Sarabhai Medal in 2016, and Science award of Ministry of Mister of Education of Japan in 2015. He is now Editor-in-Chief of IJACSA and IJISA. http://teagis.ip.is.saga-u.ac.jp/index.html